Advanced Vehicle Motion Control of EV Based on Electric Motor's Advantages

Takashi Koike
Yoshifumi Aoki
Xiaoxing Liu
Yoichi Hori

Department of Electrical Engineering, University of Tokyo
7-3-1, Hongo, Bunkyo-ku, Tokyo 113-8656, JAPAN
Tel: +81-3-5452-6287, Fax: +81-3-5452-6288
E-mail:koike@horilab.iis.u-tokyo.ac.jp

Abstract

Remarkable advantage of EV is the electric motor's excellent performance in motion control. This can be summarized as: (1) torque generation is very quick and accurate, (2) output torque is easily known, and (3) motor can be small enough to be installed in each wheel. Our final target is to enhance the vehicle stability by utilizing these advantages of EV.

First, in this paper, we propose a new skid prevention method for EVs utilizing effective torque (current) reduction characteristics in response to rapid increase of rotational speed of the motor. The experimental results using hardware skid simulator consists of Motor-Generator setup and actual vehicle test using UOT Cadwell EV verified the effectiveness of the method.

In the next part, we discuss about estimation and control technique of the body slip angle β, which is important for vehicle lateral motion stability. We will propose a novel β observer based on γ and side acceleration a_y measurement. To make this observer robust to parameter variation, a novel observer gain design is considered. Also, we propose the identification method of cornering power at each tire.

Experiments by using UOT March*II* and Cadwell EV proved the effectiveness of our proposed method.

Keywords: Battery Electric Vehicles, Control System, DC Motor, Vehicle Motion Control

1 Introduction

Recently, a lot of electric vehicles (EV) have been developed mainly to solve environmental and energy problems caused by the use of internal combustion engine vehicles (ICV). Some of them already have enough performance even in practical use. However, they have not yet utilized the most remarkable advantage of EV. The generated torque of electric motors can be controlled much more quickly and precisely than that of internal combustion engines.

It is well known that the adhesion characteristics between tire and road surface are greatly affected by the control of traction motor. This means that the vehicle stability and safety can be greatly improved by controlling the motor torque appropriately.

In this paper, we will propose some methods of stabilizing vehicle motion based on motor control. One is skid prevention control, and the other is lateral motion stabilization.

2 Modeling of EVs

2.1 One wheel model

When we mention about motion of vehicle, we use one wheel model. With simple one wheel model, the motion equations of wheel and chassis can be expressed in Equations (1) (2).

$$M_{\omega}\frac{dV_{\omega}}{dt} = F_m - F_d(\lambda) \tag{1}$$

$$M\frac{dV}{dt} = F_d(\lambda) \tag{2}$$

Equation (1) is the motion equation of the wheel, and the wheel is affected by the torque of the motor and reaction force from the road. Equation (2) is the motion equation of the chassis. And this F_d has nonlinear dependence on the slip ratio λ. Slip ratio is used to evaluate the "slip", and is expressed as relationship between the speed of the vehicle and the wheel.

After having achieved the friction coefficient μ- λ curve, the driving force F_d can be calculated by Equation (3).

$$F_d = \mu(\lambda)N \tag{3}$$

Where N is the normal component of reaction effecting on tires. The model of the one-wheel EV can be shown in Fig 1.

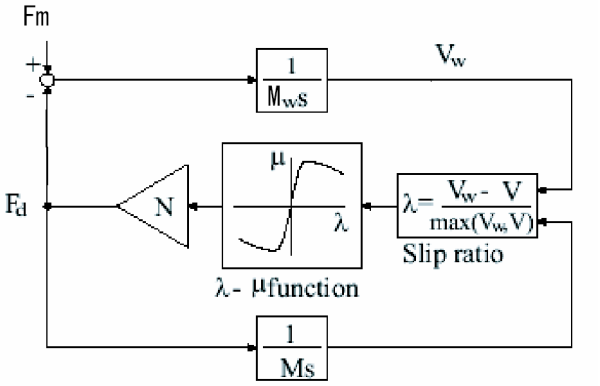

Figure 1: Block diagram of the one wheel vehicle model

2.2 Two wheel model

For two-dimensional movement of EVs, we use two-wheel model as shown in Fig 2.Generally, in order to describe vehicle's two dimension movements exactly, four-wheel model is needed. However because four-wheel model is non-linear model, it cannot be used for linear observer design.

P is the center of gravity, l_f is the distance from P to the front wheel, l_f is the distance from P to the rear wheel, α_f is the front wheel slip angle, α_r is the rear wheel slip angle and δ_f is actual steering angle at tire. Usually, we express state equations with β, γ, and vehicle speed V, which are expressed in Equation (4), where N is the yaw-moment which is generated between the left and right drive wheel. C_f and C_r are cornering power CP, which is defined as Equation (5), where F_{y_f} and F_{y_r} are each front and rear wheel's force in y direction.

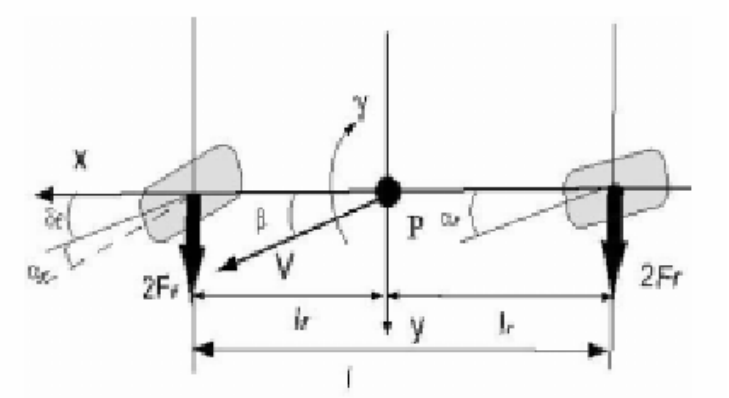

Figure 2: Two-wheel model of vehicle motion

$$\dot{x} = Ax + Bu \tag{4}$$

$$A = \begin{pmatrix} \dfrac{-(C_{fl}+C_{fr}+C_{rl}+C_{rr})}{mv} & \dfrac{-l_f(C_{fl}+C_{fr})+l_r(C_{rl}+C_{rr})}{mv^2}-1 \\ \dfrac{-l_f(C_{fl}+C_{fr})+l_r(C_{rl}+C_{rr})}{I} & \dfrac{-{l_f}^2(C_{fl}+C_{fr})+{l_r}^2(C_{rl}+C_{rr})}{Iv} \end{pmatrix}$$

$$B = \begin{pmatrix} \dfrac{C_{fl}+C_{fr}}{mv} & 0 \\ \dfrac{l_f(C_{fl}+C_{fr})}{I} & \dfrac{1}{I} \end{pmatrix}, x = \begin{pmatrix} \beta \\ \gamma \end{pmatrix}, u = \begin{pmatrix} \delta \\ N \end{pmatrix}$$

$$C_f = \frac{\partial F_f}{\partial \alpha_f}\Big|_{\alpha_f=0}, C_r = \frac{\partial F_r}{\partial \alpha_r}\Big|_{\alpha_r=0} \tag{5}$$

3 Skid Prevention Control

3.1 Skid Prevention based on Back-EMF Observer

First, we propose a novel skid prevention control method [1]. It is well-known that the separately-excited DC motor has effective torque (current) reduction characteristics in response to rapid increase of the rotational speed of the motor. This characteristic has been utilized in adhesion control of electric locomotives with DC motor.

When the vehicle is running from the dry road to the icy road, the friction between the tire and the road is rapidly reduced. If the motor of the EV is still keeping the driving torque as is commanded, the wheel will skid on the icy road quickly. That means the Back-EMF of the motor increases instantly at the same time. In other words, we can restrain the vehicle in the safe condition by decreasing the

excessively increased Back-EMF.

We propose a novel skid prevention control method as shown in Figure 3 [2].Back-EMF observer is utilized to estimate the extra increased Back-EMF which is evaluated by how much the real Back-EMF is bigger than the estimated value.

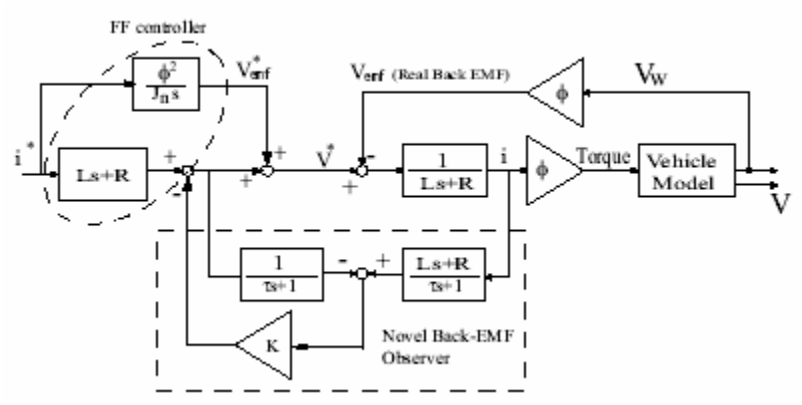

Figure 3: The Block diagram of the Back EMF observer

3.2 Experimental Results using M-G set

We did experiments about the proposed method by Motor-Generator Setup in laboratory [2]. Result of experimentation is shown in Figure 4. The motor current and the rotational speed are observed when the vehicle slips at speed acceleration. The inertia moment of the motor which is simulating the skid phenomenon decreases rapidly at about *t=2[s]*.

Figure 4(a) shows that the motor current reduces when the inertia moment decreases if the proposed controller is utilized. Therefore, the rotational speed of the motor is prevented from rapid increase in Figure 4(b).

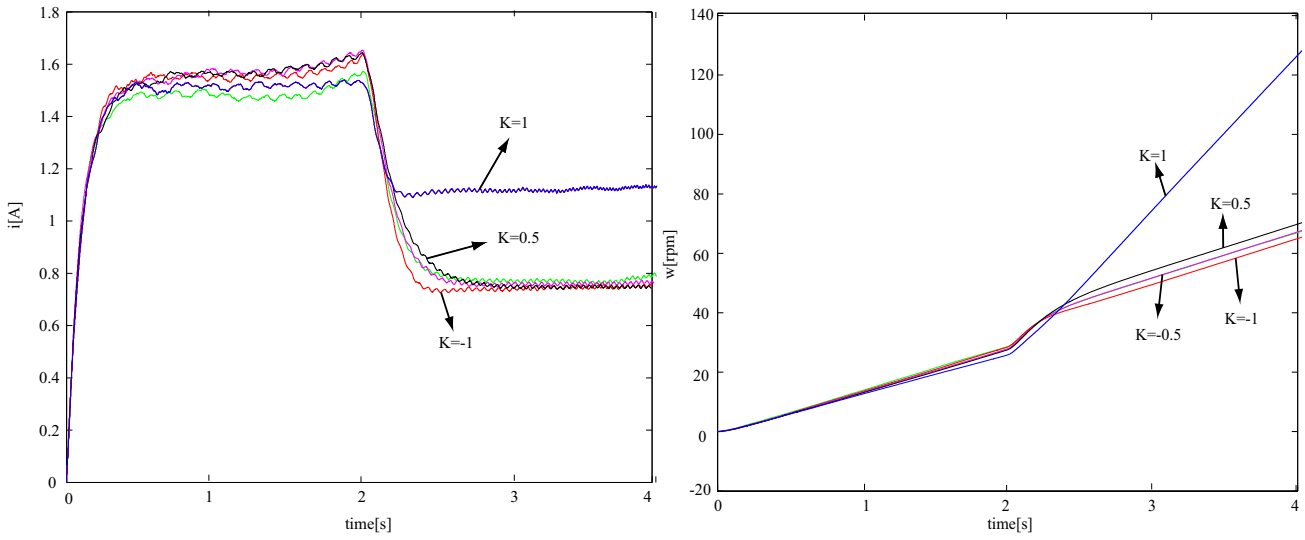

(a)Current of the motor reduces with different with different value of the gain K

(b) Rotational speed of the motor with different with different value of the gain K

Figure 4: Experimental results of the skid phenomenon with gain K (τ=*0.01*)

3.3 Experimental Results using Cadwell EV

Figure 5:Cadwell

We did another experiment about torque reduction Characteristics in response to rapid increase of the rotational speed of the motor using Cadwell EV (Figure 5) [3].

Before we did another experiment, it is necessary to equipped with BLDC motors, because Cadwell has two BLDC motors in rear wheels. The equivalent circuit of BLDC motor is expressed in Equation (6).

$$\begin{pmatrix} v_d \\ v_q \end{pmatrix} = \begin{pmatrix} R_a + pL_d & -\omega_{re}L_q \\ \omega_{re}L_d R_a & +pL_q \end{pmatrix} \begin{pmatrix} i_d \\ i_q \end{pmatrix} + \begin{pmatrix} 0 \\ \omega_{re}\psi_a \end{pmatrix} \tag{6}$$

Where R_a is armature resistance. Φ_a is magnetic flux. d and q mean d-axis and q-axis.

In order to realize the slipping control which likes previously proposed, two filers are added composing the usual vector control of BLDC motor. Figure 6 shows the vector control configuration of the EV system equipped with BLDC motor. And Figure 7 shows the block diagram of the EV system equipped with decoupling controlled BLDC motor. From this figure, G_q (s) the transfer function v_q^* to i_q and G_d (s) the transfer function from v_d^* to i_d are obtained by Equation (7).

$$G_q(s) = \frac{i_q}{v_q^*} = \frac{1}{L_q s + R_a + \dfrac{P_n^2 \psi_a^2}{Js}} \simeq \frac{J}{P_n^2 \psi_a^2} \frac{s}{1+\tau_m s} \qquad \left(\tau_m = {JR_a}\Big/{P_n^2 \psi_a^2}\right)$$

$$G_d(s) = \frac{i_d}{v_d^*} = \frac{1}{L_d s + R_a} \tag{7}$$

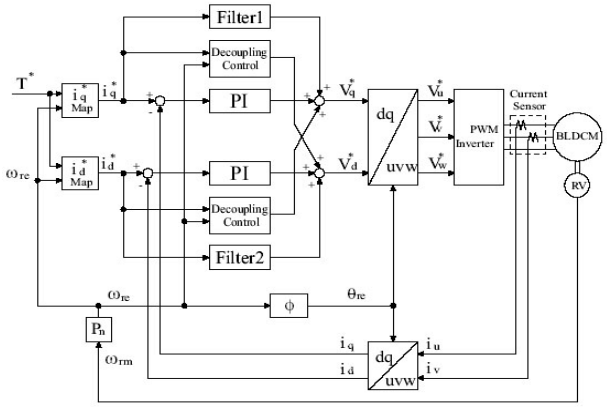

Figure 6: Vector control configuration of the EV system equipped with BLDC motor

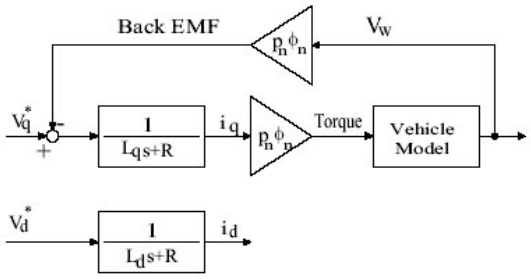

Figure 7: Block diagram of the EV system equipped with decoupling controlled BLDC motor

In Equation (7), we use approximation assuming electrical time constant is far smaller than mechanical time constant.

And there is only q axis torque element that takes part in the calculation of vector control, filter F is defined by Equation (8).

$$F = \begin{pmatrix} Filter1 \\ Filter2 \end{pmatrix} = \begin{pmatrix} G_q^{-1}(s) \\ 0 \end{pmatrix} = \begin{pmatrix} \frac{P_n^2 \psi_a^2}{J} \frac{1}{s} + R_a \\ 0 \end{pmatrix} \tag{8}$$

In experiments, we inputted constant torque command into EV, and the vehicle went into skiddy road (wet aluminum plate) from dry road (dry asphalt road).

Results of experiments are shown in Figure 8. Figure 8(a) shows that the rotational speed of motor rapidly increases without control when slip occurs. In contrast, “in with control case ", we can restrain rapid increase of the rotational motor speed as is shown in Figure 8(b).

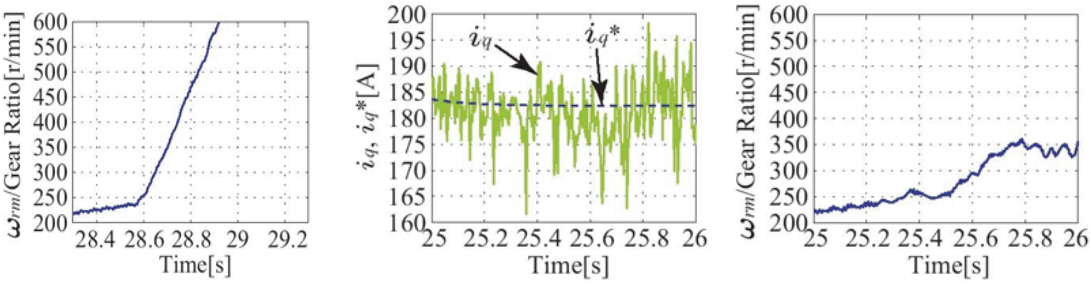

(a) Without Control (b) With skid prevention control

Figure 8: Experimental results of skid prevention control

4 Lateral Motion Stabilization

4.1 Lateral Motion Stabilization based on Body Slip Angle Observer

4.1.1 Design of proposed linear observer

Next we propose novel methods to stabilize vehicle lateral motion. Body slip angle β is important for vehicle lateral motion stability. However as sensors to measure β are very expensive, we need to estimate β from only variables to be measurable. In order to observe β, many methods have been proposed. All these methods have some disadvantages. For example, models used in some methods are too complex[4][5], some observers are not robust enough against disturbance and model error, or cannot exactly estimate β. Most approaches to design β based only on γ cannot give correct estimation.

To improve these disadvantages, we propose full order linear observer as shown in Figure 9 [6].And we can define this observer as Equation (9) (10).

$$\dot{\hat{x}} = A\hat{x} + Bu - K(\hat{y} - y) \tag{9}$$

$$\hat{y} = C\hat{x} + Du \tag{10}$$

The estimation error equation $e = \hat{\beta} - \beta$ should satisfy the following error equation (Equation (11)).

$$\dot{e} = (A - KC)e \tag{11}$$

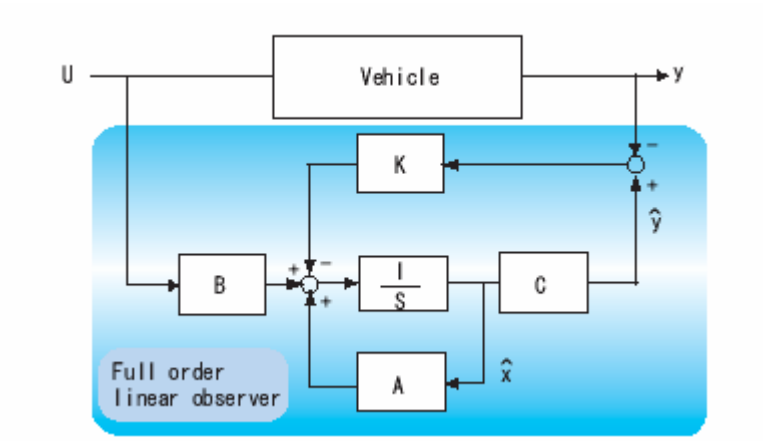

Figure 9: Full order linear observer

Full order observer's characteristic is decided by matrix gain K. If the selected matrix gain K is inadequate, the linear observer may have a poor robust performance against model error and sometimes cannot estimate β exactly. To decide the matrix gain, we must consider two important factors.

First, all eigenvalues of the proposed observer must be located in stable region. The positions of these eigenvalues will affect control system's time response performances, such as overshoot, rising time and settling time.

Second, we must design the observer robust against model error. Since two-wheel model is used in our design, some model error exists more or less. Especially, cornering power depend on road condition and loads on each tires.

To make the observer robust, we referred [6]. And a_y can be expressed as Equation (12) using Equation (4).

$$a_y = v(a_{11}\beta + a_{12} + b_1\delta + \gamma) \tag{12}$$

By calculate Equation (12), we can get $\hat{\beta}$, and we can get $\dot{\hat{\beta}}$ from Equation (13).

$$\dot{\hat{\beta}} = a_{11}\hat{\beta} + a_{12}\hat{\gamma} + b_{11}\delta_f - k_{11}(\gamma - \gamma) - k_{12}(\hat{a}_y - a_y) \tag{13}$$

State equation of β is expressed as:

$$\dot{\beta} = a'_{11}\beta + a'_{12}\gamma + \beta'_{11}\delta_f \tag{14}$$

$a'_{11}, a'_{12}, b'_{11}$ are real values. Any model error is not contained in this equation.

By Equation (13) (14), the state equation for $\hat{\beta} - \beta$ is given by following equation.

$$\dot{\hat{\beta}} - \dot{\beta} = a_{11}(1 - k_{12}v)(\hat{\beta} - \beta) + [a_{12} - k_{12}v(a_{12} + 1) - k_{11}](\hat{\gamma} - \gamma)$$
$$- (1 - k_{12}v)(a'_{11} - a_{11})\beta - (1 - k_{12}v)(a'_{12} - a_{12})\gamma - (1 - k_{12}v)(b'_{11} - b_{11})\delta_f \tag{15}$$

The best condition for robustness in Equation (15) is:

$$1 - k_{12}v = 0 \Leftrightarrow k_{12} = \frac{1}{v} \tag{16}$$

Based on consideration of pole assignment and robustness against cornering power, K is decided as:

$$K = \begin{pmatrix} \dfrac{[l_f(C_{fr} + C_{fl}) - l_r(C_{rr} + C_{rl})]\lambda_1\lambda_2 I}{(C_{fr} + C_{fl})(C_{rr} + C_{rl})(lf - lr)^2} - 1 & \dfrac{1}{v} \\ -\lambda_1 - \lambda_2 & \dfrac{m((C_{fr} + C_{fl})lf^2 - (C_{rr} + C_{rl})lr^2)}{((C_{fr} + C_{fl})lf - (C_{rr} + C_{rl})lr]I} \end{pmatrix} \tag{17}$$

λ_1, λ_2 are the assigned poles of the observer.

Therefore, utilizing redundancy in matrix gain, we made the observer robust to cornering stiffness.

4.1.2 Proposed method of cornering power identification

Additionally, from linear equation of vehicle motion, we propose the method of lateral force estimation at each tire. Cornering power CP can be identified from estimated side forced using Equation (18) and fixed trace method [7].

$$F_y = C_f \alpha \tag{18}$$

Lateral forces are estimated by Equation (20), which is derived from linear equation of vehicle motion shown as Equation (19).

$$I\dot{\gamma} = 2F_{fr}l_f \cos\delta_f - 2F_{yr}l_r + N$$
$$ma_y = 2F_{yf}\cos\delta_f + 2F_{yr} \tag{19}$$

$$\hat{F}_{yf} = \frac{I\dot{\gamma} + ml_r a_y - N}{2(l_f + l_r \cos\delta_f)}$$
$$\hat{F}_{yr} = \frac{-I\dot{\gamma} + ma_y l_f + N\cos\delta_f}{2(l_r \cos\delta_f + l_f)} \tag{20}$$

Lateral forces are also defined by Equation (21).

$$F_y = \mu(\lambda_y)F_z \tag{21}$$

And F_z are defined by Equation (22), are average normal components of reaction at front and rear tires.

$$F_{z\_f} = \frac{m(l_r g - ha_x)}{2(l_f + l_r)}, F_{z\_r} = \frac{m(l_r g + ha_x)}{2(l_f + l_r)} \tag{22}$$

Moreover, F_z can be calculated by Equation (23), where h is the distance from P to the ground.

$$\begin{aligned} F_{z\_fr} &= \frac{m(l_r g - ha_x)}{2(l_f + l_r)} + \frac{hma_y}{d}, F_{z\_fl} = \frac{m(l_r g - ha_x)}{2(l_f + l_r)} - \frac{hma_y}{d} \\ F_{z\_rr} &= \frac{m(l_r g + ha_x)}{2(l_f + l_r)} + \frac{hma_y}{d}, F_{z\_rl} = \frac{m(l_r g + ha_x)}{2(l_f + l_r)} + \frac{hma_y}{d} \end{aligned} \tag{23}$$

From Equations (20) ~ (23), we can get lateral force at each tire.

$$\begin{aligned} \hat{F}_{y\_fr} &= \mu(\lambda_{y\_f}) F_{z\_fr} = \mu(\lambda_{y\_f}) F_{z\_f} \frac{F_{z\_fr}}{F_{z\_f}} = \hat{F}_{yf}(1 + \frac{2(\hat{l}_f + l_r) ha_y}{d(l_r g - ha_x)}) \\ \hat{F}_{y\_fl} &= \mu(\lambda_{y\_f}) F_{z\_fl} = \mu(\lambda_{y\_f}) F_{z\_f} \frac{F_{z\_fl}}{F_{z\_f}} = \hat{F}_{yf}(1 - \frac{2(\hat{l}_f + l_r) ha_y}{d(l_r g - ha_x)}) \\ \hat{F}_{y\_rr} &= \mu(\lambda_{y\_r}) F_{z\_rr} = \mu(\lambda_{y\_r}) F_{z\_r} \frac{F_{z\_rr}}{F_{z\_r}} = \hat{F}_{yr}(1 + \frac{2(\hat{l}_f + l_r) ha_y}{d(l_r g - ha_x)}) \\ \hat{F}_{y\_rl} &= \mu(\lambda_{y\_r}) F_{z\_rl} = \mu(\lambda_{y\_r}) F_{z\_r} \frac{F_{z\_rl}}{F_{z\_r}} = \hat{F}_{yr}(1 - \frac{2(\hat{l}_f + l_r) ha_y}{d(l_r g - ha_x)}) \end{aligned} \tag{24}$$

4.1.3 Structure of estimating body slip angle

We estimate body slip angle β by proposed observer based on γ and a_y with cornering power identification. This is shown in Figure 10, using this estimated cornering power, estimated $\hat{\beta}$ and cornering power can complement each other. From this, better estimation of body slip angle $\hat{\beta}$ is performed.

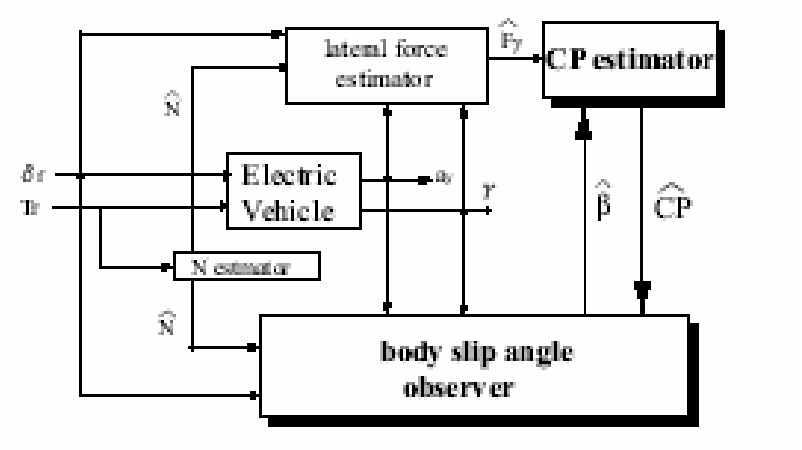

Figure 10: Cornering power estimator

4.2 Experimental Results

Figure 11: UOT March *II*

We did experiments by using UOT March*II* (Figure 11). This experimental vehicle was made for study of advanced motion control of EV driven by four inwheel motors.

We made this EV by ourselves, which is remodeling of Nissan March. In experiments, we controlled β based on DYC (Direct Yaw Moment control), which is actualized PID controller and MFC (Model Following Control) [8].

Figure 12 is the experimental results in linear region. Speed is 40[km/h] and driver's input steering wheel angle δ is 150[deg]. Figure 12(a) shows that the estimated and measured body slip angle β is suppressed by the DYC control, and Figure 12(b) depicts the identified cornering power. This figure demonstrates the effectiveness of the proposed control. Moreover, estimated β corresponds with measured β . This figure demonstrates that the novel proposed observer can estimate β in linear region even if β is strongly controlled.

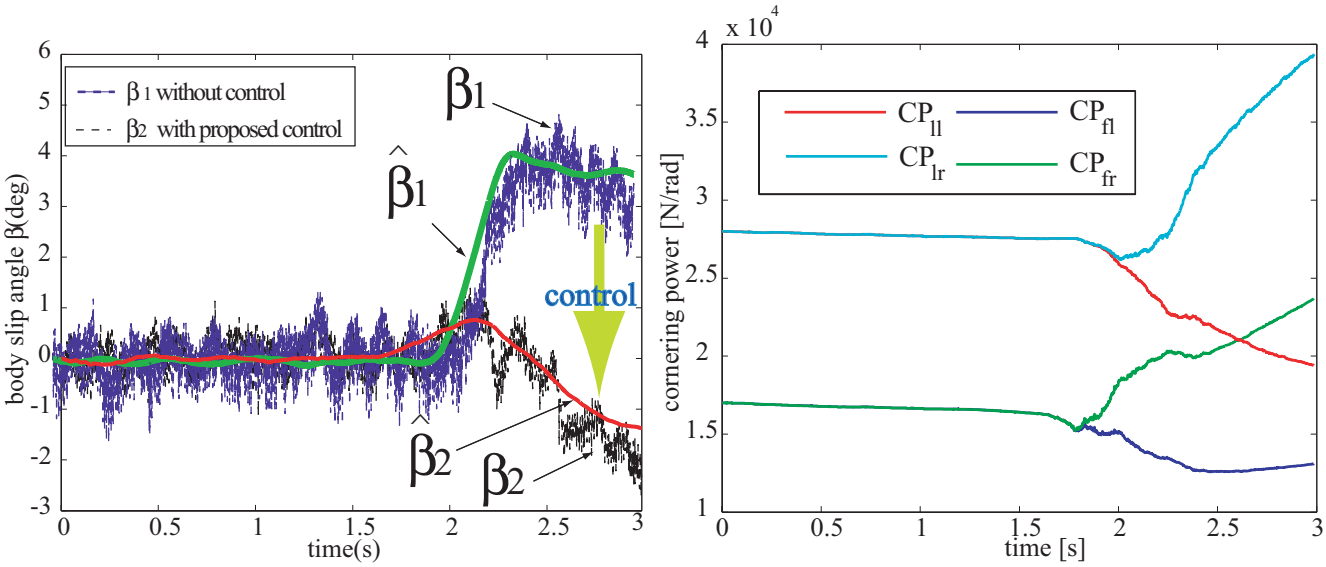

(a)comparison β with normal and proposed control (b)identified cornering power

Figure 12: β control and estimation results

5 Conclusion

In this paper, we proposed the skid prevention control for EVs utilizing Back-EMF observer and the methods to estimate β while identifying the cornering power and to control β.

Effectiveness of skid prevention control has been confirmed by the experimental results using Motor-Generator setup and Cadwell EV. For this, we can widely improve the longitudinal vehicle motion control.

And experimental results of UOT March *II* proved the effectiveness of the proposed β estimating method and show us that the proposed linear observer can estimate β under the novel control in any region. For this, we can improve lateral vehicle motion control.

These proposed methods describe the great advantage of EVs in motion control. In the future, pure EVs will become more popular and contribute to solving energy problems. It is important to pursue the researches on making full use of pure EV's advantages.

References

[1] Shinya Kodama, Lianbing Li and Yoichi Hori, "Skid Prevention for EVs based on the Emulation of Torque Characteristics of Separately-wound DC Motor", Proc of AMC 2004 pp75-80, 2004.
[2] Xiaoxing Liu, Takashi Koike, Yoichi Hori, "Skid Prevention for EVs based on Back-EMF Observer and its Implementation to IPM Motor Driven EV", AMC 9th,2005

[3] Xiaoxing Liu, Lianbing Li, Yoichi Hori, Toru Akiba, Ryota Shirato, "Optimal Traction Control for EV utilizing Fast Torque Response of Electric Motor", The 31th Annual Conference of the IEEE Industrial Electronics Society,2005

[4] Aleksander D.Rodic and Minmir K.Vukobratovic, "*Contribution to the Integrated Control Synthesis of Road Vehicles*", IEEE Transactions on Control Systems Technology Vol7 No.1, 1999.

[5] Laura R. Ray,"Nonlinear Tire Force Estimation and Road Friction Identification Simulation and Experiments", Automatica Vol.33 No.10 pp.1819-1833, 1997.
[6] Tomoko Inoue, Yoichi Hori , " Observer Design of Body Angle β for Future Vehicle Control and Experimental Equation using the Four-Motored Electric Vehicles",EVS20,2003.

[7] Yoshifumi Aoki, Zhao Li, Yoichi Hori, "Robust Design of Body Slip Angle Observer with Cornering Power Identification at Each Tire for Vehicle Motion Stabilization ", AMC 9th, 2005

[8] Shinichiro Sakai, Hideo Sado and Yoichi Hori: "Motion Control in an Electric Vehicle with Four Independently Driven In-Wheel Motors",IEEE Trans on Mechatronics Vol.4 No.1 pp.9-16, 1999.

Author

Takashi Koike, Department of Electrical Engineering University of Tokyo, 7-3-1Hongo, Bunkyo-ku, Tokyo 113-8656, JAPAN
Tel +81-3-5452-6287 Fax: +81-3-5452-6288, e-mail:koike@horilab.iis.u-tokyo.ac.jp
He received B.S. degree in Electrical Engineering from the University of Tokyo in 2006. He is now 1st-year master's degree student at the University of Tokyo and studies about EVs' motion control.

Yoshifumi Aoki, Department of Electrical Engineering University of Tokyo, 7-3-1Hongo, Bunkyo-ku, Tokyo 113-8656, JAPAN
Tel +81-3-5452-6287 Fax: +81-3-5452-6288, e-mail:y-aoki@horilab.iis.u-tokyo.ac.jp
He received M.S. degree in Electrical Engineering from the University of Tokyo in 2006. And now, he is working at Nissan Motor Co., Ltd since this April.

Xiaoxing Liu, Department of Electrical Engineering University of Tokyo, 7-3-1Hongo, Bunkyo-ku, Tokyo 113-8656, JAPAN
Tel +81-3-5452-6287 Fax: +81-3-5452-6288, e-mail:ryu@horilab.iis.u-tokyo.ac.jp
He received M.S. degree in Electrical Engineering from the University of Tokyo in 2006. And now, he is working at Tohmatsu Consulting Co., Ltd since this April.

Yoichi Hori, The Institute of Industrial Science the University of Tokyo, 4-6-1 Komaba Meguro-ku Tokyo 153-8505, Japan
Tel: +81-03 5452 6289, Fax: +81-03 5452 6288, e-mail: hori@iis.u-tokyo.ac.jp,
He received Ph.D degrees in Electrical Engineering from the University of Tokyo in 1983 and joined the Department of Electrical Engineering as a Research Associate. He later became a Professor in 2000. In 2002, he moved to the Institute of Industrial Science as a Professor of Information & Electronics Division. His research fields are control theory and its industrial application to motion control, mechatronics, robotics, electric vehicle, etc. He worked as Treasurer of IEEE Japan Council and Tokyo Section during 2001-2002. He is now an AdCom member of IEEE-IES. He was the Vice President of IEE-Japan IAS in 2004-2005. He has been the chairman of ECaSS Forum since 2005. He is the program chairperson of EVS-22. IEEE Fellow.